Arab J Geosci (2013) 6:3865–3876
DOI 10.1007/s12517-012-0647-x

ORIGINAL PAPER

Effects of mineralogical and textural characteristics of ilmenite concentrate on synthetic rutile production

A. Mehdilo · M. Irannajad

Received: 27 February 2012 / Accepted: 31 July 2012 / Published online: 15 August 2012

Abstract The effect of mineralogy and texture of Qara-aghaj ilmenite concentrate on titanium dioxide prepared via reduction-slagging acid leaching process as a raw material in chloride route was investigated. The concentrate contains 44.5 % TiO_2 and its content in ilmenite lattice varies from 41.6–48 %. Hematite exsolved lamellae inside ilmenite which affect the reduction process positively are host of the most of the Cr and V as pigment colorizer metals. Apatite fine inclusions inside ilmenite as the source of Ca and P could have negative effects on synthetic rutile. Spinel ultrafine particles inside ilmenite containing Al and Si could also affect the synthetic rutile negatively. The other important elements which have been substituted in ilmenite lattice are Mg and Mn. The prepared titanium dioxide concentrate containing 91 % TiO_2 and 0.6 % Fe_2O_3 is mainly formed by rutile and small amount of anatase and Ti_2O_3 phases. The solid solution of rutile inside Ti_2O_3 was also observed. The content of Cr, V, Mn, and Al are decreased to permissible amount during slagging and leaching process while the quantity of other impurities such as Mg, Si, and Ca are relatively high in the product, and they cause some difficulties in pigment production via chloride route. The Mg and Ca sourced from ilmenite lattice and apatite inclusions, respectively, can affect the precipitation process. So, it is predicted that Qara-aghaj ilmenite concentrate will be suitable for sulfate route, but it is necessary to investigate comprehensively.

Keywords Mineralogy · Ilmenite · Synthetic rutile · Chloride process · TiO_2 pigment

A. Mehdilo · M. Irannajad (✉)
Department of Mining and Metallurgical Engineering,
Amirkabir University of Technology,
Tehran, Iran
e-mail: iranajad@aut.ac.ir

A. Mehdilo
e-mail: amehdilo@aut.ac.ir

Introduction

Titanium is relatively abundant in the earth's crust, which is usually found in igneous and metamorphic rocks as ilmenite ($FeTiO_3$), rutile (TiO_2), and titanomagnetite (Fe_2TiO_4–Fe_2O_4). A survey on the use of titanium in its various forms indicates that almost 95 % of its use is for the production of white TiO_2 pigment which has extensive application in paint, plastic, and paper industries (Nayl et al. 2009a, b). Titanium dioxide also has high potential applications in environmental purification, gas sensors, and in photovoltaic cells due to its unique characteristics (Zhang et al. 2009). Relatively minor quantities are used to produce the metal and titanium chemicals (Lasheen 2004).

Natural rutile, owing to its high titanium content and low levels of impurities, has traditionally been preferred as feed stock for the production of titanium dioxide pigment. Natural rutile is becoming scarcer and consequently more costly, and the alternative method that uses ilmenite is being favored. Ilmenite concentrates have relatively low titanium content (usually about 50 % titanium dioxide compared to about 96 % in the case of rutile) but have Fe as their major impurity and thus pose problems for pigment production. Nevertheless, ilmenite has been used as an alternate feed material for production of pigment through chemical routes (Samala et al. 2009).

Commercial production of TiO_2 pigment uses either the sulfate process or the chloride process. In the former process, relatively low grade feedstock can be used, but it gives a higher volume of waste product that requires proper treatment and disposal. It is more preferable to use the chloride process which utilizes a feedstock of high TiO_2 grade as natural rutile mineral (94–98 % TiO_2), synthetic rutile (92–95 % TiO_2), anatase (90–95 % TiO_2), leucoxene (>68 % TiO_2), or titanium slag (80–90 % TiO_2) as raw materials (El-Hazek et al. 2007; Lasheen 2008; Nayl et

Table 1 Typical specification of slag used in the chloride process (mass percentages)

Composition	Total TiO_2	Ti_2O_3	FeO	MnO	MgO	SiO_2	Al_2O_3	CaO	V_2O_5	Cr_2O_3
wt%	>85.0	<35.0	<12.0	<2.0	<1.2	<2.0	<1.5	<0.13	<0.60	<0.25

al. 2009b; Samala et al. 2009; Zhang and Nicol 2010). The chloride process offers several advantages such as the yield of high quality products, a more eco-friendly process, and the generation of a smaller amount of waste products (Zhang and Nicol 2010).

The shortage of natural rutile and the need for higher grade titanium feedstocks has encouraged ilmenite upgrading by removing iron oxide and other impurities from the grain lattice, thus converting ilmenite into synthetic rutile for the chlorination process (Mahmoud et al. 2004; El-Hazek et al. 2007; Lasheen 2009). There are several processes for the production of synthetic rutile from ilmenite, and some of them were commercially applied. One of these processes is smelting processes, where the iron part of the ilmenite is reduced and melted to separate the iron from titanium. The titanium slag is then leached with the sulfuric acid or with hydrochloric acid at elevated temperatures (Lasheen 2004; Mahmoud et al. 2004; Kamala et al. 2006; El-Hazek et al. 2007; Sasikumar et al. 2007; Li et al. 2008; Lasheen 2009; Zhang and Nicol 2010).

The titanium slag produced from this process represents an important feedstock for the manufacture of titanium dioxide pigment by the sulfate process (Olanipekun 1999). One of the major constraints for using chloride process is the slag composition. The reason for this is that the chlorination process can handle only low levels of impurities. The typical specification of slag used in the chloride process is presented in Table 1 (Pistorius 2008). So, the crucial factors which affect the reactions of pigment production via sulfate and chloride processes are mineral and chemical composition of the feed and its textural features. Ilmenite is known to contain the trace elements Cr, V, Mn, Mg, Nb, and Ta. The Cr, V, and Nb affect the pigment color, and their presence may reduce the value of concentrate as pigment plant feed. Mg affects the precipitation process; Ca and P cause problems in the crystallization process (Chernet 1999). Also, the impurities such as MgO and CaO affect the stability of the fluidized bed: the boiling points of $MgCl_2$ and $CaCl_2$ (the reaction products of MgO and CaO during chlorination) are above the chlorination temperature, and so these chlorides accumulate in the fluidized bed (Pistorius 2008). Partly due to the need to produce good quality pigment but also due to environmental pressure regarding waste disposal, pigment producers are forced to use feedstock with a low level of trace elements (Chernet 1999).

For applying the chloride process with more advantages, the titanium-rich slag is further acid-leached by a hydrometallurgical process. As a leachant, hydrochloric acid is preferred to other acids because it allows comparatively easier recovery of the useful free acid from its waste solution. In addition, the recovery of a number of metal ions by liquid–liquid extraction from hydrochloric acid solutions is considerably easier than that from sulphuric acid solutions (Olanipekun 1999).

Beside Kahnoj beach sands in the south of Iran (Irannajad 1990), Qara-aghaj hard rock deposit which is located 36 km away from Urmia in Azarbayejan province northwest of Iran, has recently been explored and studied as another titanium resource. The studied area is close to the Iran–Turkey border and considered as a part of the Khoy-Mahabad structural subzone. Indeed, this area can be considered as a junction of three main structural zones including those of Alborz-Azerbaijan, Central Iran, and Sanandaj-Sirjan. The main host rocks of the Fe-Ti-P bearing ore body is Qareaghaj mafic-ultramafic intrusion (QMUI) including wehrlite and lherzolite with minor clinopyroxenite. The

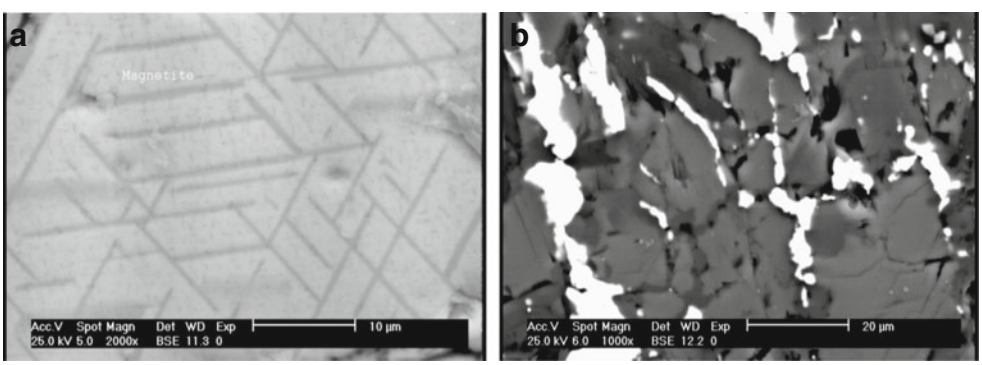

Fig. 1 **a** Ilmenite lamellae inside magnetite (titanomagnetite). **b** Dissemination of ilmenite inside silicate minerals

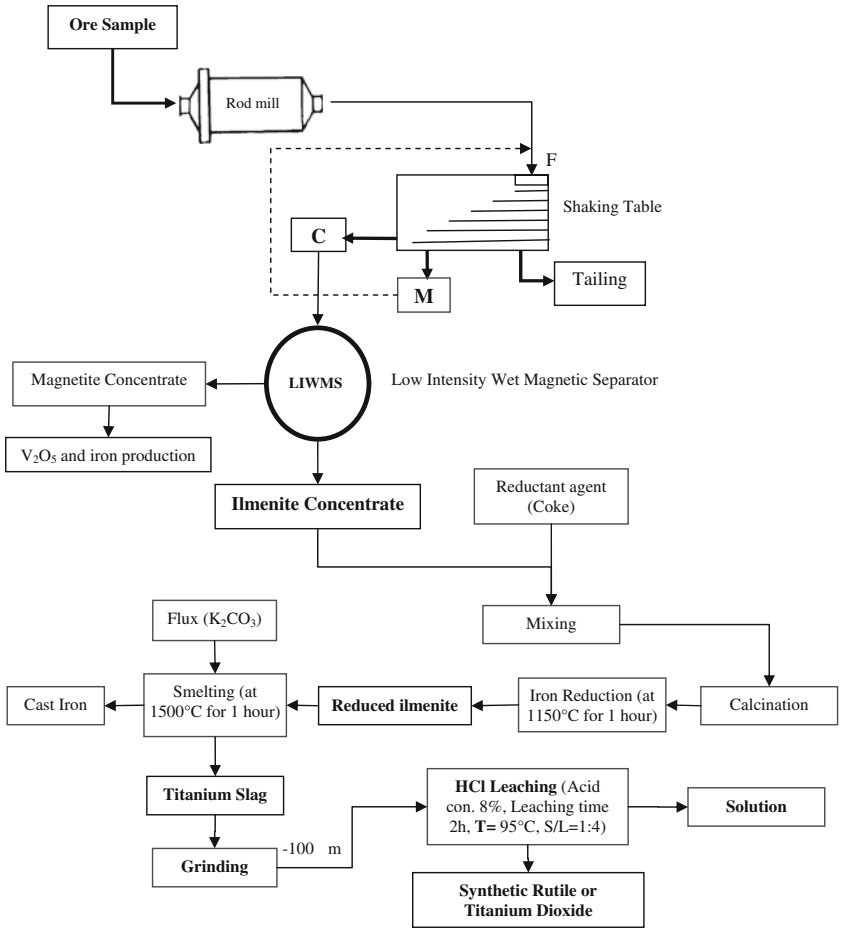

Fig. 2 Schematic diagram of ilmenite concentrate production, ilmenite reduction, slagging, and acid leaching process

QMUI is composed mainly of nonmineralized mafic and apatite- and Fe-Ti oxide-rich ultramafic rocks. The mafic rocks, mainly coarse-grained gabbro, microgabbro, and amphibolite, have a simple mineral assemblage (plagioclase + clinopyroxene + ilmenite) and based on field observations, mineralogy and chemical composition are comagmatic. The ultramafic rocks contains high proportion of olivine (~40–66 vol%), apatite (~0.1–16 vol%), ilmenite (~11–19 vol%), and magnetite (~2–13 vol%). The QMUI as a small igneous body is situated between Permian and Infracambrian–Cambrian

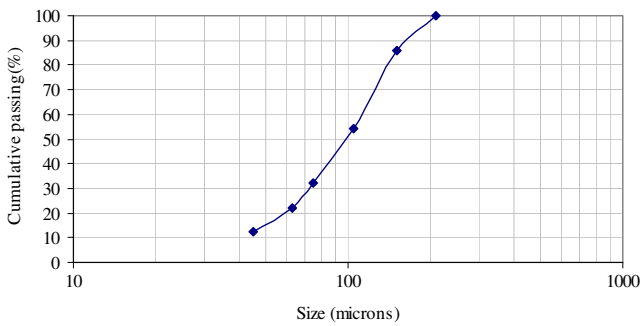

Fig. 3 Particle size distribution of ilmenite concentrate

sequences, composed mainly of sedimentary and low-grade metamorphic rocks on the north and Precambrian metamorphic complexes to the south and east. The Infracambrian–Cambrian rocks include Barut and Zaigun Formations, Lalun sandstone, Mila dolomite and limestone, mainly located on the north of the QMUI. The Permian, red quartzo-feldspathic sandstone (Durud Formation), and limestone-dolomitic limestone (Ruthe Formation) have a fault contact with the northern margin of the QMUI. Triassic and Jurassic sequences are absent, while Cretaceous rocks include thick sequences of flysch and the Khoy ophiolitic complex. The youngest, Quaternary, rocks and sediments are composed of andesitic-basaltic lavas, travertine terraces and gravel fans, mainly located in the northwest (Mehdilo 2003; Mirmohammadi et al. 2007; Yaghubpur et al. 2007).

In the Qara-aghaj ore, titanium occurs mainly in the form of ilmenite partly as separated grains, exsolved lamellae in magnetite (Fig. 1a) and dissemination in silicate minerals (Fig. 1b). Pyroxene, olivine, and plagioclase are the main gangue minerals. The laboratory investigations indicated that only the grains form of ilmenite could be beneficiated by physical separation methods, while the lamellae and disseminated forms with the sizes finer than 20 μm are not

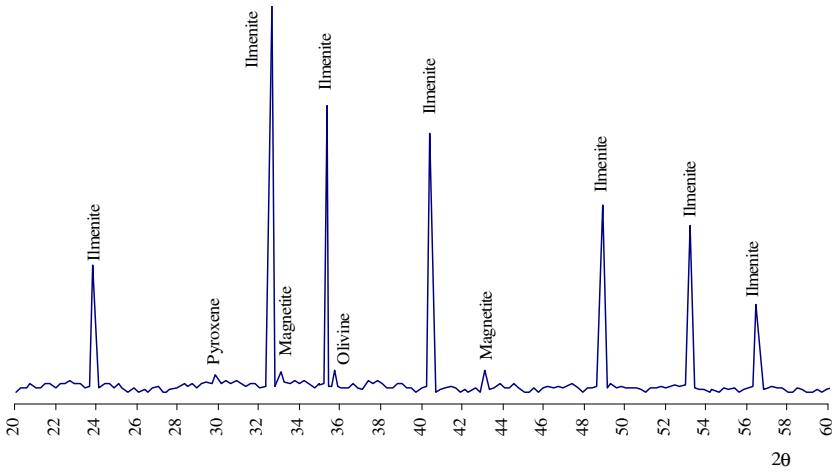

Fig. 4 XRD pattern of ilmenite concentrate

Table 2 Chemical composition of ilmenite concentrate

Composition	TiO_2	Fe_2O_3	MnO	V_2O_5	P_2O_5	CaO	MgO	SiO_2	Al_2O_3	Cr_2O_3
wt%	44.5	46.1	0.83	0.26	0.21	0.68	3.76	2.57	0.58	0.42

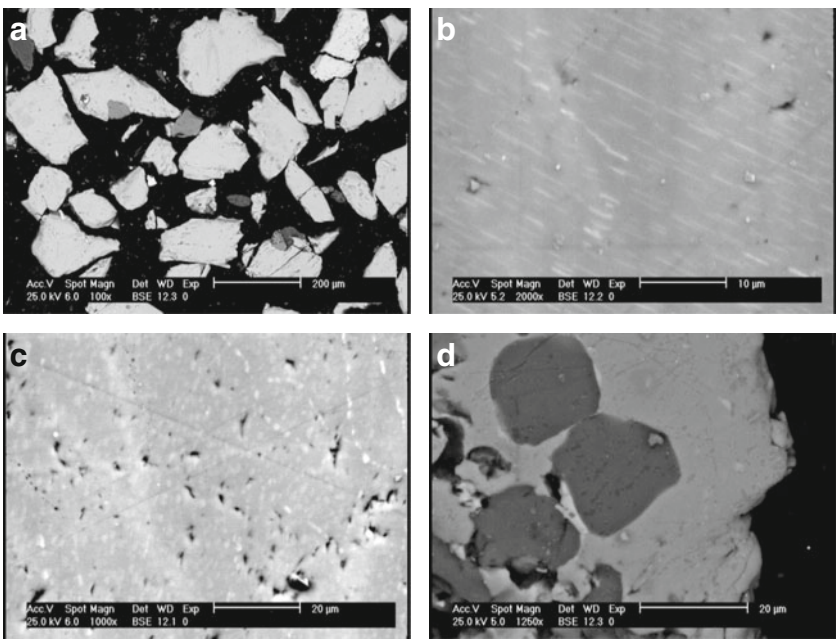

Fig. 5 Mineralogical and textural features of ilmenite taken by SEM (BSE detector). **a** Ilmenite grains of concentrate and some locked and free grains of gangue minerals. **b** Hematite exsolved lamellae inside ilmenite. **c** Hematite exsolved fine particles inside ilmenite. **d** Apatite inclusion inside ilmenite

Table 3 Selected EDX analysis of ilmenite, ilmenite lamellae and apatite

Point	Phase	Composition (wt%)											
		TiO_2	Fe_2O_3	MnO	V_2O_5	P_2O_5	CaO	MgO	SiO_2	Al_2O_3	Cr_2O_3	F	Total
1	Ilmenite	43.45	50.97	1.48	0.36	–	–	0.59	1.15	1.28	0.42	–	99.7
2	Ilmenite	41.6	47.25	1.13	0.38	0.92	0.22	2.06	2.51	2.92	0.45	–	99.44
3	Ilmenite	47.34	48.08	0.85	0.40	0.35	0.2	0.75	0.98	0.61	–	–	99.56
4	Ilmenite	48.0	48.99	0.95	0.45	0.21	0.09	–	0.96	–	0.1	–	99.85
5	Ilmenite	45.42	47.58	1.19	0.37	1.31	0.28	0.56	1.15	0.68	0.21	–	98.75
6	Ilmenite	42.28	50.75	1.15	0.42	0.21	0.36	2.4	1.16	0.95	0.24	–	99.92
7	Ilmenite	42.5	48.49	1.25	0.35	0.31	0.39	2.41	2.15	1.9	0.23	–	99.98
8	Ilmenite	45.47	48.75	1.14	0.42	0.38	0.34	0.91	1.19	0.55	0.27	–	99.42
9	Ilmenite	46.51	49.96	0.74	0.42	0.25	0.16	0.56	0.89	0.47	–	–	99.96
10	Ilmenite	46.53	49.92	1.02	0.39	–	0.06	0.38	0.97	0.37	–	–	99.64
11	Ilmenite	46.21	49.25	1.42	0.38	–	0.08	0.65	0.92	0.78	–	–	99.69
12	Ilmenite	46.76	49.44	1.38	0.35	–	0.27	–	1	0.41	0.22	–	99.83
13	Ilmenite	46.06	48.89	1.19	0.44	0.08	0.26	1.49	0.77	0. 66	0.16	–	99.34
14	Ilmenite	46.29	47.67	1.3	0.33	–	0.2	1.62	1.21	0.9	0.11	–	99.63
15	Ilmenite	41.75	53.29	1.32	0.24	0.14	0.4	0.75	1.18	0.66	–	–	99.73
16	Light lamellae	33.7	58.42	1.15	0.78	1.08	0.37	0.91	1.49	1.4	0.48	–	99.88
17	Light lamellae	35.58	58.42	1.15	1.07	–	0.27	1.18	1.36	0.52	0.38		99.93
18	Light grains	28.86	68.07	1.2	0.69	–	0.42	–	0.55	–	0.18	–	99.97
19	Light grains	31.29	59.55	0.82	0.98	0.24	0.35	2.25	2.62	1.45	0.35	–	99.86
20	Apatite	0.39	1.26	–	0.19	39.8	54.1	–	1.48	–	–	2.71	99.93
21	Apatite	0.29	0.94	0.37	0.32	40.3	53.07	0.96	1.03	0.54	–	2.14	99.96
22	Spinel (dark grain)	1.4	58.99	0.34	0.85	3.86	0.21	4.89	1.08	27.9	0.43	–	99.95
23	Spinel (dark grain)	15.92	34.25	0.76	0.45	–	–	7.8	1.81	38.56	0.44	–	99.99

recoverable by these methods. Based on the laboratory test results, the combination of gravity and magnetic separation (Fig. 2) has been suggested for production of ilmenite concentrate (Mehdilo 2003; Irannajad and Mehdilo 2004, 2007; Mehdilo and Irannajad 2010). Also, reducing-smelting acid leaching process according in Fig. 2 has been proposed for production of titanium dioxide or synthetic rutile as feed material of chloride process (Mehdilo 2003; Irannajad and Montajam 2005; Mehdilo and Irannajad 2006; Mehdilo et al. 2006).

In this research, the effects of mineralogical and chemical characteristics of Qara-aghaj ilmenite concentrate and its textural features on prepared synthetic rutile via reduction-smelting acid leaching process are investigated.

Materials and methods

The materials used in this study were ilmenite concentrate, reduced ilmenite, titanium slag, and titanium dioxide which were prepared according in Fig. 2. The chemical and mineralogical compositions of these materials were carried out using X-ray fluorescence (XRF) and X-ray diffraction (XRD). Polished sections were studied using optical

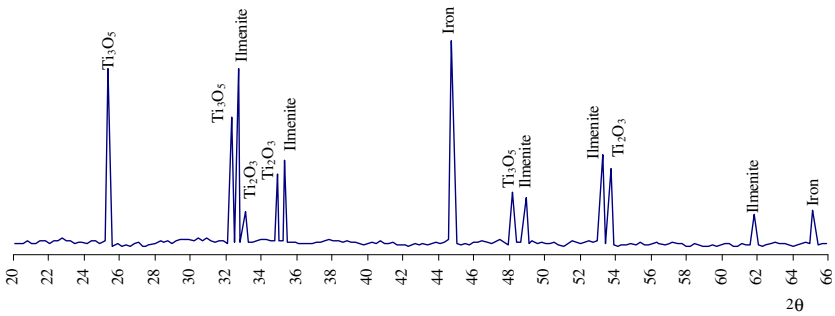

Fig. 6 XRD pattern of reduced ilmenite

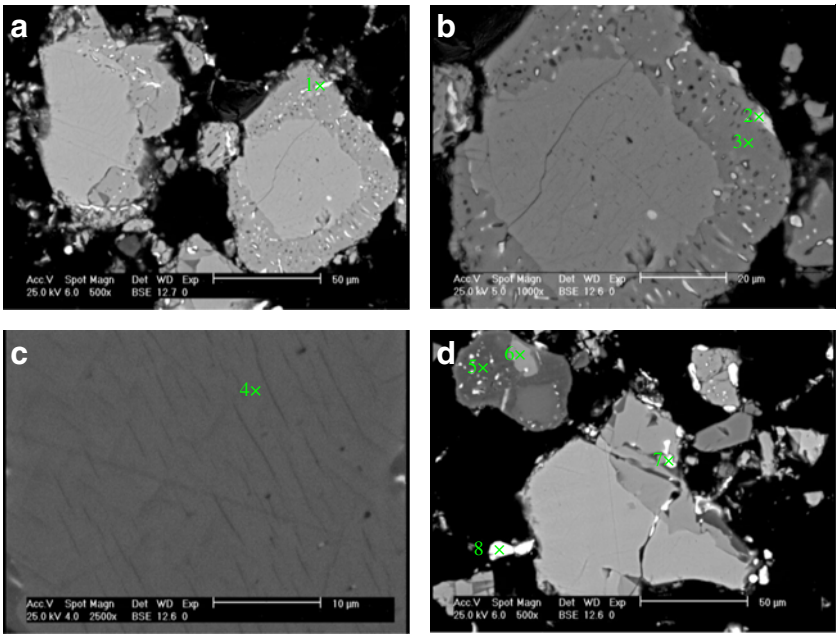

Fig. 7 Mineralogical and textural features of reduced ilmenite taken by SEM (BSE detector). **a** Reduced particles of ilmenite. **b** Ilmenite reduction and formation of secondary oxide phase. **c** The oriented pits inside ilmenite due to reduction and forward out of hematite lamellae. **d** Reduction of ilmenite particles and forward out of metallic iron

Table 4 Selected EDX analysis of reduced ilmenite

Spot no.	Analyzed points	Composition (wt%)										
		TiO_2	Fe_2O_3	MnO	V_2O_5	P_2O_5	CaO	MgO	SiO_2	Al_2O_3	Cr_2O_3	Total
1	Light particles (Fig. 7a)	10.02	85.48	0.65	0.35	0.34	0.05	0.6	0.81	1.04	0.35	99.69
2	Light particles (Fig. 7b)	26.1	69.9	0.72	0.35	0.42	0.11	0.3	1.29	0.28	0.31	99.78
3	Reduced Ilmenite (Fig. 7b)	66.64	27.16	1.13	0.30	0.51	0.33	2.12	1.10	0.19	0.3	99.78
4	Reduced ilmenite (dark part, Fig. 7c)	55.02	36.61	2.45	0.19	0.52	0.13	2.23	1.41	0.99	0.44	99.99
5	Reduced ilmenite (dark part, Fig. 7d)	70.14	20.66	2.51	0.21	0.5	0.35	3.83	0.64	0.7	0.43	99.97
6	Reduced ilmenite (gray part, Fig. 7d)	55.08	34.6	1.43	0.45	0.59	0.3	2.71	3.48	1.04	0.21	99.89
7	Light particles (Fig. 7d)	7.25	86.26	0.55	0.14	0.39	0.00	0.22	4.41	0.46	0.24	99.92
8	Light particles (Fig. 7d)	8.49	87.98	0.43	0.2	0.12	0.08	0.49	0.8	0.94	0.2	99.73

Table 5 Chemical composition of titanium slag

Composition	TiO_2	Fe_2O_3	MnO	MgO	SiO_2	Al_2O_3	V_2O_5	CaO	P_2O_5	Cr_2O_3	K_2O	Total
%wt	72.7	7.8	0.97	3.21	5.24	2.80	0.30	1.08	0.45	0.37	4.22	99.8

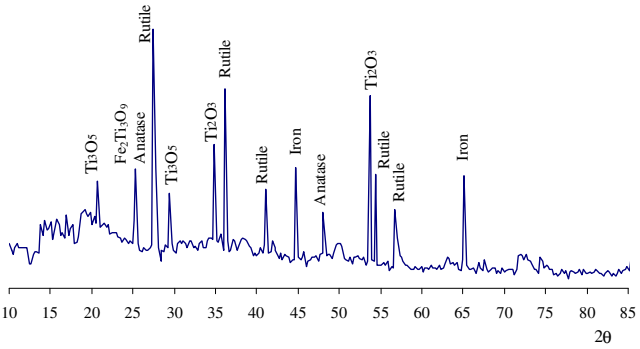

Fig. 8 XRD pattern of titanium slag used as raw material in acid leaching

microscopy and scanning electron microscopy (Philips, model XL30) equipped with EDX. Microscopical observations were made on various features including alteration, exsolutions, grain sizes, grain shapes, fracturing, grain locking, pores, and other textural factors. The chemical composition and trace element constituents on each phase, on minute exsolutions and on inclusions were determined using EDX. The mechanical sieving was applied to study the particle size distribution.

Results and discussion

Characterization of ilmenite concentrate

The grain size distribution of ilmenite concentrate is given as shown in Fig. 3, from which it is evident that about 88 % of ilmenite ranges from 210 to 45 μm. XRD pattern of ilmenite concentrate and its chemical composition analyzed by XRF are shown in Fig. 4 and Table 2, respectively. The results indicate that the concentrate by grading of 44.5 % TiO_2 contain about 90 % ilmenite which is comparable with commercially available ilmenite concentrates in the world. The other minerals in the concentrate are magnetite and minor amount of hematite and some silicate minerals.

Back-scattered electron (BSE) images prepared using scanning electron microscopy is shown in Fig. 5, and the analysis of different ilmenite particles and other phases performed by EDX is given in Table 3. Figure 5a shows the ilmenite-liberated grains in the concentrate. Also, some locked and free grains of gangue minerals such as pyroxene and olivine are observed. The content of gangue or rock-forming minerals (mainly pyroxene) in the concentrate does not exceed 5 %. The other mineral which is observed in ilmenite concentrate is magnetite as locked particles. Figure 5b, c show that hematite is in the form of exsolved lamellae, and particles range in size from 0.1 to 1 μm inside ilmenite. Hematite lamellae are generally considered to represent solid state exsolution of originally homogeneous hematite–ilmenite solid solutions. These lamellae appear when the Fe_2O_3 content of the initial solid solution exceeds 7–9 mole%, above 18 wt% Fe_2O_3 (Duchesne 1970; Chernet 1999). The abundance of exsolutions varies widely from grain to grain. The analysis of these lamellae by EDX (Table 3, rows 16–19) indicated that these lamellae could be hemoilmenite.

It can be seen that ilmenite grains enclose exsolution bodies of hematite. It also reveals that minute hematite lamellae are segregated, forming elongated bodies of hematite within the ilmenite host. Thus, the ore is mainly formed from ferri-ilmenite together with small quantities of titanohematite. Based on the EDX analysis, the TiO_2 content of

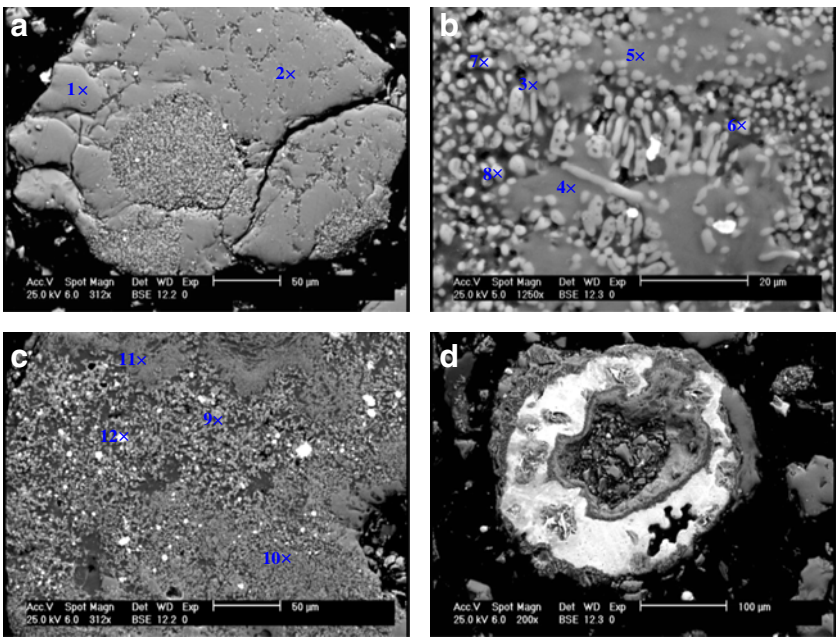

Fig. 9 Mineralogical and textural features of titanium slag taken by SEM (BSE detector). **a** BSE image of crushed titanium slag; partial transformation of slag to titanium rich phases. **b** Titanium-rich phases of image a with higher magnification. **c** Presence of pig iron particles inside titanium slag. **d** A larger grain of pig iron surrounding a titanium slag grain

Table 6 Selected EDX analysis of titanium slag

Spot no.	Analyzed points	Composition (wt%)										
		TiO_2	Fe_2O_3	MnO	V_2O_5	P_2O_5	CaO	MgO	SiO_2	Al_2O_3	Cr_2O_3	Total
1	Compact parts of slag (spot 1, Fig. 9a)	69.42	0.61	0.57	–	0.69	0.16	17.91	0.62	9.84	0.16	99.98
2	Compact parts of slag (spot 2, Fig. 9a)	70.45	0.44	1.18	0.20	0.75	2.40	4.55	13.40	6.32	0.27	99.96
3	Pseudorutile (Fig. 9b)	75.46	0.49	0.44	–	0.55	1.95	10.50	4.02	6.22	0.33	99.96
4	Pseudorutile (Fig. 9b)	77.72	0.55	1.17	–	0.44	2.24	0.97	12.66	3.92	0.32	99.98
5	Pseudorutile (Fig. 9b)	77.61	0.31	0.94	–	2.03	1.05	8.92	5.09	3.78	0.22	99.95
6	Spherical particles (rutile or anatase) (spots 6, 7, 8; Fig. 9b) (spots 9, 10; Fig. 9c)	89.24	0.51	0.28	–	0.77	0.72	2.63	0.61	4.95	0.26	99.96
7		90.43	0.78	1.0	0.25	1.05	–	3.96	0.74	1.15	0.62	99.97
8		88.32	0.71	0.58	0.07	0.51	0.14	5.95	0.87	2.43	0.38	99.96
9		88.67	0.81	0.44	0	0.60	1.51	0.85	4.64	2.22	0.22	99.96
10		85.71	0.8	0.67	–	0.73	0.37	7.27	0.28	3.70	0.43	99.96
11	Compact parts of slag (Fig. 9c)	65.69	4.13	0.53	–	–	3.94	8.24	8.94	8.14	0.34	99.95
12	Light grains, iron (Fig. 9c)	4.60	90.53	0.33	0.17	0.85	0.13	0.60	1.11	0.95	0.71	99.98

ilmenite (41.6–48.0 %) is lower than the theoretical ilmenite composition (52.6 %). The maximum amount of TiO_2 in ilmenite lattice is 48 %. So, the maximum content of ilmenite in the concentrate with average grading of 44.5 % TiO_2 could be 92.7 % approximately. Since the term ilmenite, as used in the titanium industry, commonly covers the entire range from unweathered ilmenite with TiO_2 contents below 50 % to altered ilmenite containing more than 60 % TiO_2 (Chernet 1994), so there is no ilmenite alteration in Qara-aghaj deposit. The higher content of Fe_2O_3 in ilmenite lattice can be due to the presence of hematite in solid solution or as fine exsolution lamellae in ilmenite. The MgO and MnO contents of ilmenite are 0.74–1.48 and 0.38–2.4 %, respectively, which are relatively high. Considering the given contents of MnO and MgO, the ilmenite has more of pyrophanite and geikielite component. A trace amount of Cr_2O_3 and V_2O_5 is locally present in the ilmenite lattice (0.0–0.45 %). However, it was found that hematite lamellae or hemoilmenite is the host of most of the vanadium (0.69–1.07 wt% V_2O_5) and chromium (0.18–0.48 % Cr_2O_3).

Some apatite fine particles (mainly lower than 30 μm) are observed as inclusion form inside ilmenite (Fig. 5d). According to the analysis of apatite by EDX (Table 3, rows 20 and 21), the fluorine content (2.14–2.71 wt%) is indicative of fluorapatite composition. Rarely, ilmenite also contains oriented dark lamellae of spinel which are evidenced by analysis using EDX (Table 3, rows 22 and 23). Al_2O_3 is an indicator for the presence of spinel.

The quality of ilmenite concentrate can be affected by exsolved hemoilmenite lamellae or hematite solid solution in ilmenite, spinel lamellae, apatite inclusions, and by the abundance of elements in the ilmenite lattice. Presence of Mn and Mg can affect the pigment production process. The quantity of V and Cr in the ilmenite is low; however, their presence may reduce the value of concentrate as pigment production feed.

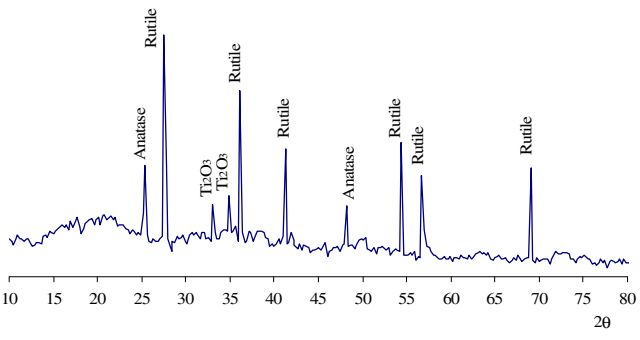

Fig. 10 XRD pattern of prepared titanium dioxide concentrate

Characterization of reduced ilmenite

Reduction of ilmenite concentrate was studied at different conditions, and the optimum amount of temperature and time as two crucial parameters were determined at 1,150 °C and 1 h, respectively.

According in Fig. 6, XRD revealed the presence of phases such as $FeTiO_3$, Ti_3O_5, Ti_2O_3, and metallic iron. The back-scattered images of ilmenite reduction were obtained with SEM and are shown in Fig. 7. The light particles are metallic iron and iron carbide, which is produced by reduction of iron oxides at the earlier stages of reduction process. The partial reduction of Ti^{4+} to Ti^{3+} forming a secondary oxide phase also took place in this stage. With proceeding of reduction reactions, some Ti^{3+} is converted to Ti^{2+}. The metallic phase consisting mainly of iron was observed as globules dispersed within the simultaneously formed secondary oxide phase that formed the outer rim of shrinking-core-type of reduction process (Fig. 7a, b).

Table 7 Chemical composition of produced titanium dioxide

Composition	TiO_2	Fe_2O_3	MnO	MgO	SiO_2	Al_2O_3	V_2O_5	CaO	K_2O	Cr_2O_3	Cl	Total
Percentage	91.0	0.60	0.62	2.11	3.56	0.86	0.18	0.58	0.09	0.20	0.19	99.99

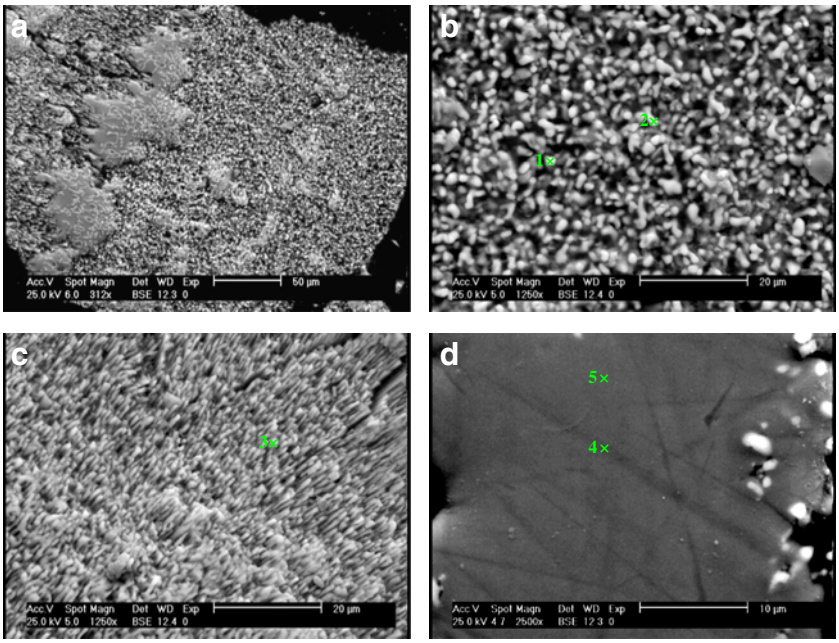

Fig. 11 Textural and morphological characteristics of titanium dioxide particles prepared by hydrochloric acids leaching at the optimum conditions. **a** Synthetic rutile produced by HCl leaching. **b** Synthetic rutile elongated grains with clear boundaries. **c** Needle-like crystals of synthetic rutile. **d** Exsolution of rutile inside Ti2O3

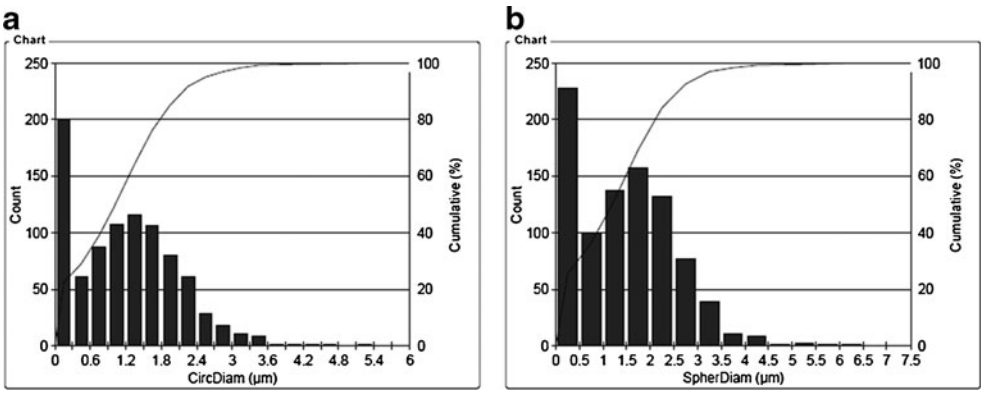

Fig. 12 Size distribution of titanium dioxide particles produced by HCl leaching. **a** Circular diameter. **b** Spherical diameter

Table 8 Information about size distribution of particles produced by HCl leaching

Diameter	Minimum size (μm)	Maximum size (μm)	Mean size (μm)	D_{80} (μm)	Standard Deviation (μm)
Circular	0.1	5.2	1.2	1.95	0.849
Spherical	0.2	6.3	1.47	2.31	1.04

Figure 7c shows that all of the hematite lamellae inside ilmenite disappeared and forwarded out as metallic iron due to its higher reduction kinetics than ilmenite and now appear as oriented pits. The reduction of ilmenite proceeded not only from grain boundaries but also from these pits. These oriented pits affect the reduction of ilmenite positively. So, the hematites lamellae do not have negative effects on next stages of titanium dioxide production and then chlorination process.

Point analyses using EDX indicate that the metallic phase formed at earlier stages contained mostly iron with little titanium (Table 4, points 1, 2, 7, and 8). The oxide phase regions near the metallic phase contained high titanium and low iron due to outward diffusion of Fe^{2+} towards the surface resulting in reduction to metallic iron (Table 4, points 3 and 5). The center of particles or regions far from the metallic iron reduced less than the outer layers of the particles have low titanium content (Table 4, points 4 and 6). The results presented here are qualitatively in good agreement with the earlier results of Merk and Pickles (1988), Gupta et al. (1990), Welham and Williams (1999), and Kucukkaragoz and Eric (2006).

Characterization of titanium slag

The chemical and phase composition of the titanium slag is shown in Table 5 and Fig. 8, respectively. By comparison of chemical composition of produced slag with typical slag used in the chloride process (Pistorius 2008), it is found that this slag with low content of TiO_2 and high level of impurities is not suitable for pigment production through chloride process. However, after slagging, Fe_2O_3 content of the slag has been decreased until 7.8 %, but it is the most important of all impurities which should be removed. Fe_2O_3 is mainly in the form of iron metal which could not be separated from the slag. The other impurities are mainly light elements such as Si, Mg, Al, Ca, P, and K which are concentrated in the slag product. The contents of Mn and V are relatively low, but Cr content is higher than permissible amount. SiO_2 and some of MgO and Al_2O_3 are sourced from silicate minerals and spinel lamellae inside ilmenite. MnO and some of MgO are related to impurities in ilmenite lattice. P_2O_5 and CaO are sourced from apatite inclusions inside ilmenite. Cr and V as colorizers of pigment are resulted in from hematite (hemoilmenite) and ilmenite lattice. The high content of K_2O in slag is due to potassium carbonate consumption as flux in slagging process. It was expected that Mn and Cr would be concentrated in the matt (iron cast), but they could not be separated from the titanium slag. XRD pattern of the slag shows that rutile is the most important phase in the sample. The other titanium containing phases are Ti_2O_3, Ti_2O_5, anatase and negligible amount pseudorutile ($Fe_2Ti_3O_9$). The impure phase of the slag was detected as FeO. The BSE images of produced slag are shown in Fig. 9, and different parts or phases were chemically analyzed by EDX (Table 6). These results indicate that some parts of the slag have been transformed to titanium-rich phases with spherical morphology (Fig. 9b) containing up to 85 % TiO_2 (Table 6). The other titanium containing phase is probably pseudorutile which has been evidenced by EDX spot analysis (Table 6). The analysis of light particles shows that they are metallic iron. These irons could be removed in the acid leaching process.

Characterization of titanium dioxide concentrate

The residue of dissolution process using HCl at optimum condition (HCl conc. 8 %, leaching time 2 h, S/L 1:4, and particle size −100 μm) was studied as synthetic rutile. The produced titanium dioxide concentrate was washed and dried. Based on the XRD results (Fig. 10), rutile is the dominant phase in this concentrate, but Ti_2O_3 and anatase phases were also found. The chemical analysis of the final product is presented in Table 7. The BSE images of produced titanium

Table 9 Selected EDX spot analysis of synthetic rutile prepared by hydrochloric acid leaching

Analyzed points	Composition (wt%)										
	TiO_2	Fe_2O_3	MnO	V_2O_5	P_2O_5	CaO	MgO	SiO_2	Al_2O_3	Cr_2O_3	Total
1	88.60	0.78	1.31	–	0.84	0.41	4.07	2.55	1.14	0.22	99.92
2	91.42	0.68	1.14	–	0.39	0.21	4.13	0.95	0.90	0.14	99.96
3	92.23	0.58	0.68	–	0.47	0.61	2.18	2.26	0.67	0.17	99.85
4	89.94	0.61	1.16	–	0.69	0.49	4.86	1.02	1.0	0.20	99.97
5	93.01	0.48	0.96	0.12	0.13	0.45	3.05	0.58	0.90	0.22	99.99

dioxide concentrate are shown in Fig. 11. A large portion of slag is destroyed by HCl and resulted in elongated grains with clear boundaries and also needle-like crystals. Some parts are undestroyed and relatively compact (Fig. 11d). Some dark lamellae are observed inside undestroyed parts. EDX analyses reveal that the TiO_2 content of lamellae (89.94 %) is less than its background (93.01 %). So the dark lamellae and background are probably rutile (TiO_2) and Ti_2O_3, respectively.

The particle size of the titanium dioxide concentrate was also determined by the image analysis method using a Clemex software. The cumulative percent of particles as a function of circular and spherical diameter is shown in Fig. 12. The information about size distribution is presented in Table 8.

The chemical analysis indicates that the final titanium dioxide concentrate contains about 91 % TiO_2 and only 0.6 % iron as Fe_2O_3. The content of other impurities, especially MgO, SiO_2 and CaO are relatively high. Point analysis using EDX (Table 9) shows that the maximum content of TiO_2 is 93 %, and the minimum content of iron as Fe_2O_3 is 0.48 %. Among the coloring metals, the content of V_2O_5 and Cr_2O_3 in the produced material does not exceed 0.12 and 0.22 %, respectively, but the quantity of MnO_2 by the source of ilmenite lattice varies from 0.88 to 1.31 % and could negatively affect the chlorination process. Al_2O_3 content varies from 0.68 to 1.14 and does not have negative effect on pigment process, but the content MgO, SiO_2, and CaO are out of permissible contents and could affect the chloride process negatively. These impurities are mainly the chlorine-consuming components and should be removed before using the synthetic rutile as feed of process.

Conclusion

However, Qara-aghaj ilmenite concentrate containing 44.5 % TiO_2 is comparable with some commercial concentrates in the world such as tellnes in Norway, but it has some mineralogical and textural difficulties which could have negative effects on prepared titanium dioxide for pigment production via chloride process. The intimate intergrowth of hematite with ilmenite (as solid solution forms) can take titanium into its lattice and decreases the Ti content of ilmenite. In addition of ilmenite lattice, hematite lamellae are host of most of the chromium and vanadium as pigment colorizer metals. Hematite solid solutions assist ilmenite reduction process. The creation of oriented pits inside ilmenite due to high reduction kinetic of hematite lamellae favors ilmenite reduction reaction which is more effective in iron separation and removing from ilmenite. The fine apatites (finer than 30 microns) as inclusions inside ilmenite is transformed to slag phase during smelting process and increase the Ca and P content of the titanium dioxide. The very fine particles of spinel can also increase the Al and Si content in the feed materials of the chloride process. EDX analysis indicates that ilmenite has considerable amount of Mn and Mg in its lattice probably in the composition of pyrophanite and geikielite, respectively. However, some of the Mg content is sourced from rock-forming minerals such as pyroxene and olivine.

During reduction-slagging acid leaching process, iron is removed considerably. Although the prepared titanium dioxide containing 91 % TiO_2, 0.6 % Fe_2O_3, and low levels of colorizing metals especially V and Cr is more suitable raw material for pigment production through chloride process, but the high quantity of some impurities such as Si, Mg, Ca, and maybe Mn create some problems. Mg and Ca are the chlorine-consuming components and affect the rate of TiO_2 precipitation. However, using other conditions such as alkaline leaching (Nayl et al. 2009a, b), the removing of some impurities (for example, Si or Mg and Ca) is possible, but it is necessary to investigate the applying of sulfate process for Qara-aghaj ilmenite concentrate and its titanium slag.

References

Chernet T (1994) Ore microscopic investigation of selected Fe-Ti oxides bearing samples from Konusaarenneva mineralization and other localities in South Western Finland, Geological Survey of Finland, unpublished report M10/2341/-94/1, pp. 1–25

Chernet T (1999) Effect of mineralogy and texture in the TiO_2 pigment production process of Tellnes ilmenite concentrate. Mineral Petrol 67:21–32

Duchesne JC (1970) Microtexture of Fe-Ti oxide minerals in the south rogaland anorthositic complex (Norway). Ann Soc Geol Belg 93:527–544

El-Hazek N, Lasheen TA, El-Sheikh R, Zaki SA (2007) Hydrometallurgical criteria for TiO_2 leaching from Rosetta ilmenite by hydrochloric acid. Hydrometallurgy 87:45–50

Gupta KS, Rajakumar V, Grieveson P (1990) The role of preheating in the kinetics of reduction of ilmenite with carbon. Can Metall Q 29 (1):43–49

Irannajad M (1990) Pilot plant flowsheet development of the Kahnooj titanium ore deposit, MSc Thesis, Amirkabir University of Technology,Tehran, Iran (in Farsi)

Irannajad M, Mehdilo A (2004) Concentration of Iranian titanium ore by physical methods, Minerals engineering conferences–gravity concentration 04, March 22–23, 2004, Perth, Australia

Irannajad M, Mehdilo A (2007) Laboratory-based flowsheet development of Iranian ilmenite upgrading, 20th International mining congress and exhibition of Turkey IMCET

Irannajad M, Montajam M (2005) Upgrading of ilmenite concentrate from Uromieh Qara Aghaj by smelting, 1st Iranian Mining Engineering Conference, 2–5 February, Tehran, Iran (in Farsi)

Kamala KS, Thomas CA, Devabrata M, Archana A (2006) An overview on the production of pigment grade titanium from titanium-rich slag. Waste Manag Res 24:74–79

Kucukkaragoz CS, Eric RH (2006) Solid state reduction of a natural ilmenite. Miner Eng 19:334–337

Lasheen TAI (2004) Chemical benefication of Rosetta ilmenite by direct reduction leaching. Hydrometallurgy 76:123–129

Lasheen TA (2008) Soda ash roasting of titanium slag product from Rosetta ilmenite. Hydrometallurgy 93:124–128

Lasheen TA (2009) Sulfate digestion process for high purity TiO_2 from titanium slag. Front Chem Eng China 3:155–160

Li C, Liang B, Wang HY (2008) Preparation of synthetic rutile by hydrochloric acid leaching of mechanically activated Panzhihua ilmenite. Hydrometallurgy 91:121–129

Mahmoud MHH, Afifi AAI, Ibrahim IA (2004) Reductive leaching of ilmenite ore in hydrochloric acid for preparation of synthetic rutile. Hydrometallurgy 73:99–109

Mehdilo, A (2003) Mineral processing studies of the Qara-aghaj titanium ore by physical methods, MSc Thesis, Amirkabir University of Technology, Tehran, Iran (In Farsi)

Mehdilo A, Irannajad M (2006) Production of TiO_2 pigment from Iranian titanium recourses. Iran Surf Coat Mag 15:16–22 (In Farsi)

Mehdilo A, Irannajad M (2010) Applied mineralogical studies on Iranian hard rock titanium deposit. J Miner Mater Charact Eng 9 (3):247–262

Mehdilo A, Irannajad M, Shafaei SZ (2006) Investigation about TiO_2 pigment production from ilmenite concentrate of Qarah-aghaj titanium deposit, 1st international & 2nd national conference on color science and technology, 2–5 January, 2006. Tehran, Iran (In Farsi)

Merk R, Pickles CA (1988) Reduction of ilmenite by carbon monoxide. Can Metall Q 27(3):179–185

Mirmohammadi M, Kananian A, Tarkian M (2007) The nature and origin of Fe-Ti-P-rich rocks in the Qareaghaj mafic-ultramafic intrusion. NW Iran Mineral Petrol 91:71–100

Nayl AA, Awwad NS, Aly HF (2009a) Kinetics of acid leaching of ilmenite decomposed by KOH part 2. Leaching by H_2SO_4 and $C_2H_2O_4$. J Hazard Mater 168:793–799

Nayl AA, Ismail IM, Aly HF (2009b) Ammonium hydroxide decomposition of ilmenite slag. Hydrometallurgy 98:196–200

Olanipekun E (1999) A kinetic study of the leaching of a Nigerian ilmenite ore by hydrochloric acid. Hydrometallurgy 53:1–10

Pistorius PC (2008) Ilmenite smelting: the basics. J South Afr Inst Min Metall 108:34–43

Samala S, Mohapatra BK, Mukherjee PS, Chatterjee SK (2009) Integrated XRD, EPMA and XRF study of ilmenite and titanium slag used in pigment production. J Alloys Compd 474:484–489

Sasikumar C, Rao DS, Srikanth S, Mukhopadhyay NK, Mehrotra SP (2007) Dissolution studies of mechanically activated Manavalakurichi ilmenite with HCl and H_2SO_4. Hydrometallurgy 88:154–169

Welham NJ, Williams JS (1999) Carbothermic reduction of ilmenite ($FeTiO_3$) and rutile (TiO_2). Metall Mater Trans B 30B(December):1075–1081

Yaghubpur A, Rahimsouri Y, Alipour S (2007) Mineralogy, geochemistry and genesis of titanium rich rocks of Qara Aqaj Area, Urmia, Northwest Iran. J Sci Islam Repub Iran 18(3):269–284

Zhang S, Nicol MJ (2010) Kinetics of the dissolution of ilmenite in sulfuric acid solutions under reducing conditions. Hydrometallurgy 103:196–204

Zhang Y, Qi T, Zhang Y (2009) A novel preparation of titanium dioxide from titanium slag. Hydrometallurgy 96:52–56